



Department of Electronics and Telecommunication Engineering

University of Moratuwa

BM4151 - Biosignal Processing

MATLAB Assignment 3

Continuous and Discrete Wavelet Transforms

Name

H. D. M. Premathilaka

Index

180497C

This report is submitted in partial fulfillment of the requirements for the module
BM 4151 – Biosignal Processing.

Date of Submission: January 6, 2023

Table of Contents

List of Figures	1
List of Tables	3
1 Continuous Wavelet Transform	4
1.1 Introduction	4
1.2 Wavelet Properties	4
1.2.1 Deriving the Mexican Hat Function $m(t)$	4
1.2.2 Calculating the Normalizing Factor of $m(t)$	5
1.2.3 Deriving the Generic Mexican Hat Wavelet Function	5
1.2.4 Generating Mexican Hat Daughter Wavelet Function for Different Scaling Factors	6
1.2.5 Verifying that the Wavelet Properties are Satisfied	7
1.2.6 Plotting the Spectra of the Daughter Wavelets	8
1.3 Continuous Wavelet Decomposition	9
1.3.1 Creating the Waveform $x[n]$	9
1.3.2 Applying the Scaled Mexican Hat Wavelets to $x[n]$	9
1.3.3 Visualizing the Spectrogram	9
1.3.4 Commenting on the Spectrogram	10
2 Discrete Wavelet Transform	10
2.1 Introduction	10
2.2 Applying DWT with the Wavelet Toolbox in MATLAB	10
2.2.1 Creating the Waveforms $x_1[n]$ and $x_2[n]$	10
2.2.1.1 Corrupting $x_1[n]$ and $x_2[n]$ with AWGN	11
2.2.2 Observing the Morphology of Haar and Daubechies Tap 9 Wavelets	12
2.2.3 Calculating the 10-level Decomposition of the Signal	14
2.2.3.1 10-level Decomposition of $y_1[n]$ Signal	14
2.2.3.2 10-level Decomposition of $y_2[n]$ Signal	16
2.2.4 Using Inverse DWT to Reconstruct the Signal	17
2.2.4.1 Comparing the Energies the Original and Reconstructed Noisy Signals	19
2.3 Signal Denoising with DWT	20
2.3.1 Plotting the Magnitudes of the Wavelet Coefficients	20
2.3.2 Selecting Thresholds and Reconstructing the Signals	21
2.3.3 Calculating the RMSE between the Original Signal and Denoised Signal	23
2.3.4 Repeating the Procedure with Haar Wavelets	25
2.3.5 Commenting on the Suitability of the Wavelets used	25
2.4 Signal Compression with DWT	25
2.4.1 Obtaining the Discrete Wavelet Coefficients of the ECG Signal	25
2.4.2 Finding the no. of Coefficients which Represent 99% of the Energy	27
2.4.3 Compressing the ECG Signal and Finding the Compression Ratio	27
2.4.3.1 Using the DB9 Wavelet	27
2.4.3.2 Using the Haar Wavelet	28

List of Figures

1 Mexican Hat Daughter Wavelet Function for Different Scaling Factors (First 10 Scaling Factors)	6
--	---

2	Mexican Hat Daughter Wavelet Function for Different Scaling Factors (Last 10 Scaling Factors)	6
3	Variation of Means and Energies of Mexican Hat Wavelet Function for Different Scaling Factors	7
4	Spectra of the Mexican Hat Daughter Wavelet Function for the first 10 Scaling Factors	8
5	Spectra of the Mexican Hat Daughter Wavelet Function for the last 10 Scaling Factors	8
6	$x[n]$ Signal	9
7	Spectrogram of the $x[n]$ Signal after CWT	9
8	$x_1[n]$ Signal	10
9	$x_2[n]$ Signal	11
10	$y_1[n]$ Signal	11
11	$y_2[n]$ Signal	12
12	Haar Wavelet Function and Scaling Function (Using wavefun())	12
13	DB-9 Wavelet Function and Scaling Function (Using wavefun())	12
14	Haar Wavelet Function and Scaling Function (Using waveletAnalyzer GUI) . . .	13
15	DB-9 Wavelet Function and Scaling Function (Using waveletAnalyzer GUI) . . .	13
16	Approximated Coefficients - Haar - 10 Level - $y_1[n]$ Signal	14
17	10-level Decomposition of $y_1[n]$ Signal - Haar Wavelet	14
18	Approximated Coefficients - DB9 - 10 Level - $y_1[n]$ Signal	15
19	10-level Decomposition of $y_1[n]$ Signal - DB9 Wavelet	15
20	Approximated Coefficients - Haar - 10 Level - $y_2[n]$ Signal	16
21	10-level Decomposition of $y_2[n]$ Signal - Haar Wavelet	16
22	Approximated Coefficients - DB9 - 10 Level - $y_2[n]$ Signal	17
23	10-level Decomposition of $y_2[n]$ Signal - DB9 Wavelet	17
24	Reconstructed $y_1[n]$ Signal - Haar Wavelet	18
25	Reconstructed $y_1[n]$ Signal - DB9 Wavelet	18
26	Reconstructed $y_2[n]$ Signal - Haar Wavelet	18
27	Reconstructed $y_2[n]$ Signal - DB9 Wavelet	19
28	Wavelet Coefficients for the First Wave Pair - DB9 Wavelet	20
29	Wavelet Coefficients for the Second Wave Pair - DB9 Wavelet	20
30	Wavelet Coefficients for the First Wave Pair - Haar Wavelet	21
31	Wavelet Coefficients for the Second Wave Pair - Haar Wavelet	21
32	Denoised $y_1[n]$ Signal - DB9 Wavelet	22
33	Denoised $y_2[n]$ Signal - DB9 Wavelet	22
34	Denoised $y_1[n]$ Signal - Haar Wavelet	22
35	Denoised $y_2[n]$ Signal - Haar Wavelet	23
36	$x_1[n]$ Signal and Denoised $y_1[n]$ Signal - DB9 Wavelet	23
37	$x_2[n]$ Signal and Denoised $y_2[n]$ Signal - DB9 Wavelet	24
38	$x_1[n]$ Signal and Denoised $y_1[n]$ Signal - Haar Wavelet	24
39	$x_2[n]$ Signal and Denoised $y_2[n]$ Signal - Haar Wavelet	24
40	aV_R Lead of ECG	25
41	Wavelet Coefficients of the ECG Signal: DB9 Wavelet	25
42	Wavelet Coefficients of the ECG Signal: Haar Wavelet	26
43	Compressed ECG Signal: DB9 Wavelet	26
44	Compressed ECG Signal: Haar Wavelet	26
45	Original and Compressed ECG Signal: DB9 Wavelet	27
46	Original and Compressed ECG Signal: Haar Wavelet	28

List of Tables

1	Energy Comparison between Original and Reconstructed $y_1[n]$ Signals	19
2	Energy Comparison between Original and Reconstructed $y_2[n]$ Signals	19
3	Comparison between the RMSEs under Haar and DB9 Wavelets	23
4	No. of Coefficients which Represent 99% of the Energy	27
5	Summary of Compression Results: DB9 Wavelet	27
6	Summary of Compression Results: Haar Wavelet	28

1 Continuous Wavelet Transform

1.1 Introduction

When the scaling factor is s , the translation is τ and the wavelet function is ψ , the continuous wavelet transform could be defined as,

$$W(s, \tau) = \int x(t) \frac{1}{\sqrt{s}} \psi \left(\frac{t - \tau}{s} \right) dt$$

Haar, Shannon, and Mexican hat are some of the common wavelet families and in this section, we will look into the Mexican hat mother wavelet.

1.2 Wavelet Properties

The three main properties of a wavelet $\psi(t)$ are,

- Zero mean $\implies \int_{-\infty}^{\infty} \psi(t) dt = 0$
- Unity power $\implies \int_{-\infty}^{\infty} \psi^2(t) dt = 1$
- Compact support (Bulk of the energy is concentrated within a finite time period)

1.2.1 Deriving the Mexican Hat Function $m(t)$

We know that the Gaussian function is given by,

$$g(t) = \frac{1}{\sqrt{2\pi}\sigma} \exp \left(-\frac{1}{2} \left(\frac{t - \mu}{\sigma} \right)^2 \right)$$

When the $\mu = 0$ and $\sigma = 1$, the aforementioned equation could be reduced to the following.

$$g(t) = \frac{1}{\sqrt{2\pi}} \exp \left(-\frac{t^2}{2} \right)$$

Now, let's derive the Mexican hat function.

$$\begin{aligned} m(t) &= -\frac{d^2 g(t)}{dt^2} \\ m(t) &= -\frac{d \left(\frac{dg(t)}{dt} \right)}{dt} \\ m(t) &= -\frac{d \left(\frac{d \left(\frac{1}{\sqrt{2\pi}} \exp \left(-\frac{t^2}{2} \right) \right)}{dt} \right)}{dt} \\ m(t) &= \frac{d \left(\frac{1}{\sqrt{2\pi}} t \exp \left(-\frac{t^2}{2} \right) \right)}{dt} \\ m(t) &= \frac{(1 - t^2)}{\sqrt{2\pi}} \exp \left(-\frac{t^2}{2} \right) \end{aligned}$$

1.2.2 Calculating the Normalizing Factor of $m(t)$

The Mexican hat function is symmetric about the vertical axis and therefore, has a zero mean. However, the raw Mexican hat function doesn't have a unity power and hence, could not be considered a wavelet unless normalized. In the following calculation, the derivation of the normalizing factor is given.

$$\begin{aligned}
E &= \int_{-\infty}^{\infty} m^2(t) dt \\
E &= \int_{-\infty}^{\infty} \left(\frac{(1-t^2)}{\sqrt{2\pi}} \exp\left(-\frac{t^2}{2}\right) \right)^2 dt \\
&= \frac{1}{2\pi} \lim_{L \rightarrow \infty} \left[\int_{-L}^L \exp(-t^2) dt - 2 \int_{-L}^L t^2 \exp(-t^2) dt + \int_{-L}^L t^4 \exp(-t^2) dt \right] \\
E &= \frac{1}{2\pi} \left[\sqrt{\pi} - 2 \frac{\sqrt{\pi}}{2} + \frac{3\sqrt{\pi}}{4} \right] \\
E &= \frac{3}{8\sqrt{\pi}} \neq 1
\end{aligned}$$

Accordingly, we can take the normalizing factor to be \sqrt{E} . Take the normalized Mexican hat function to be $\hat{m}(t)$. Then,

$$\begin{aligned}
\hat{m}(t) &= \frac{1}{\sqrt{E}} m(t) \\
&= \frac{2\sqrt{2}\pi^{\frac{1}{4}}}{\sqrt{3}} \frac{(1-t^2)}{\sqrt{2\pi}} \exp\left(-\frac{t^2}{2}\right) \\
\hat{m}(t) &= \frac{2}{\sqrt{3}\pi^{\frac{1}{4}}} (1-t^2) \exp\left(-\frac{t^2}{2}\right)
\end{aligned}$$

Now, we will take this result as the normalized Mexican hat wavelet function where $\psi(t) = \hat{m}(t) = \frac{2}{\sqrt{3}\pi^{\frac{1}{4}}} (1-t^2) \exp\left(-\frac{t^2}{2}\right)$.

In the next part, we will derive the generic normalized Mexican hat wavelet function including the scaling factor and translation.

1.2.3 Deriving the Generic Mexican Hat Wavelet Function

When the scaling factor is s , the translation is τ , the generic wavelet function is $\psi_{s,\tau}(t)$ could be defined as,

$$\begin{aligned}
\psi_{s,\tau}(t) &= \frac{1}{\sqrt{s}} \psi\left(\frac{t-\tau}{s}\right) \\
\psi_{s,\tau}(t) &= \frac{1}{\sqrt{s}} \left[\frac{2}{\sqrt{3}\pi^{\frac{1}{4}}} \left(1 - \left(\frac{t-\tau}{s} \right)^2 \right) \exp\left(-\frac{1}{2} \left(\frac{t-\tau}{s} \right)^2 \right) \right] \\
\psi_{s,\tau}(t) &= \frac{2}{\sqrt{3}s\pi^{\frac{1}{4}}} \left[\left(1 - \left(\frac{t-\tau}{s} \right)^2 \right) \exp\left(-\frac{1}{2} \left(\frac{t-\tau}{s} \right)^2 \right) \right]
\end{aligned}$$

1.2.4 Generating Mexican Hat Daughter Wavelet Function for Different Scaling Factors

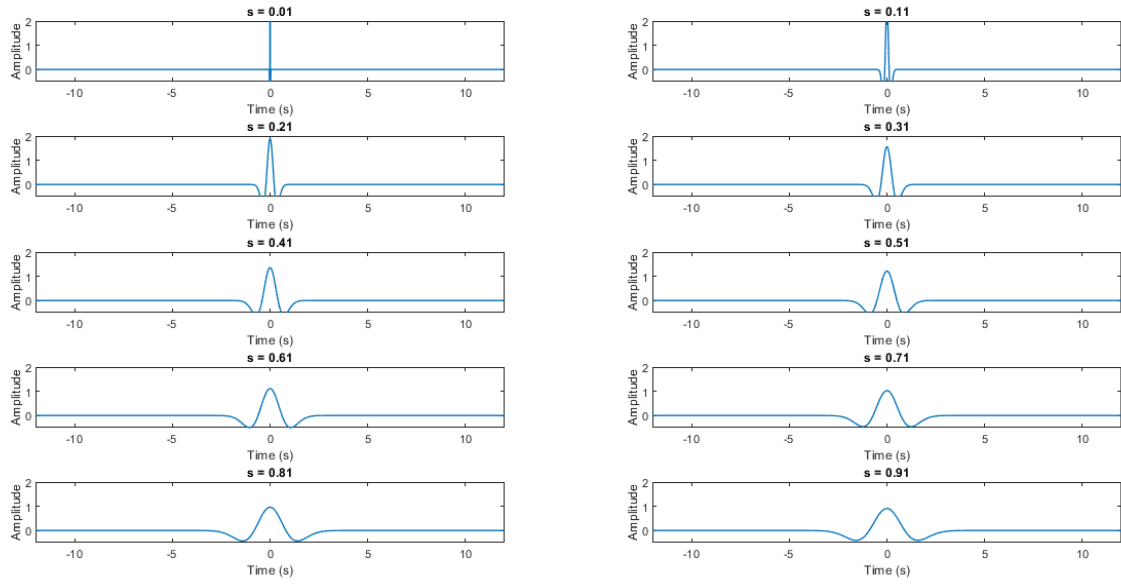


Figure 1: Mexican Hat Daughter Wavelet Function for Different Scaling Factors (First 10 Scaling Factors)

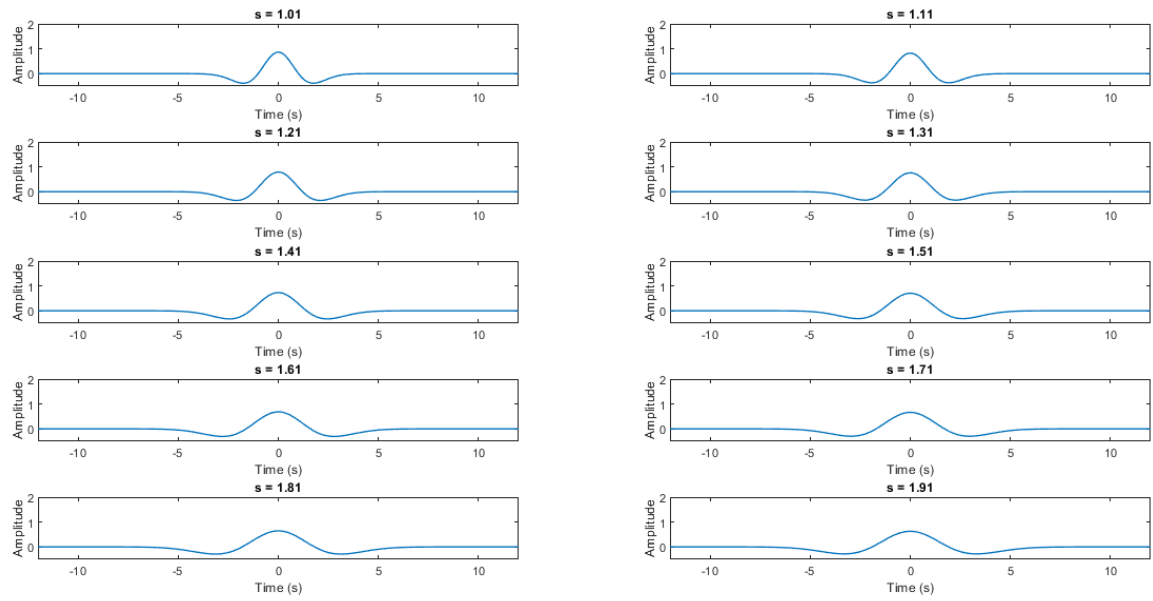


Figure 2: Mexican Hat Daughter Wavelet Function for Different Scaling Factors (Last 10 Scaling Factors)

1.2.5 Verifying that the Wavelet Properties are Satisfied

The three main properties of a wavelet $\psi(t)$ are,

- Zero mean $\implies \int_{-\infty}^{\infty} \psi(t) dt = 0$
- Unity power $\implies \int_{-\infty}^{\infty} \psi^2(t) dt = 1$
- Compact support (Bulk of the energy is concentrated within a finite time period)

From Fig. 1 and Fig. 2, we could see that the bulk of the energy is concentrated within a short span. Thus, the third criterion is satisfied. We could also see that the functions have zero mean and unity power via the plot given below. All the wavelets at different scaling factors have zero mean and unity power.

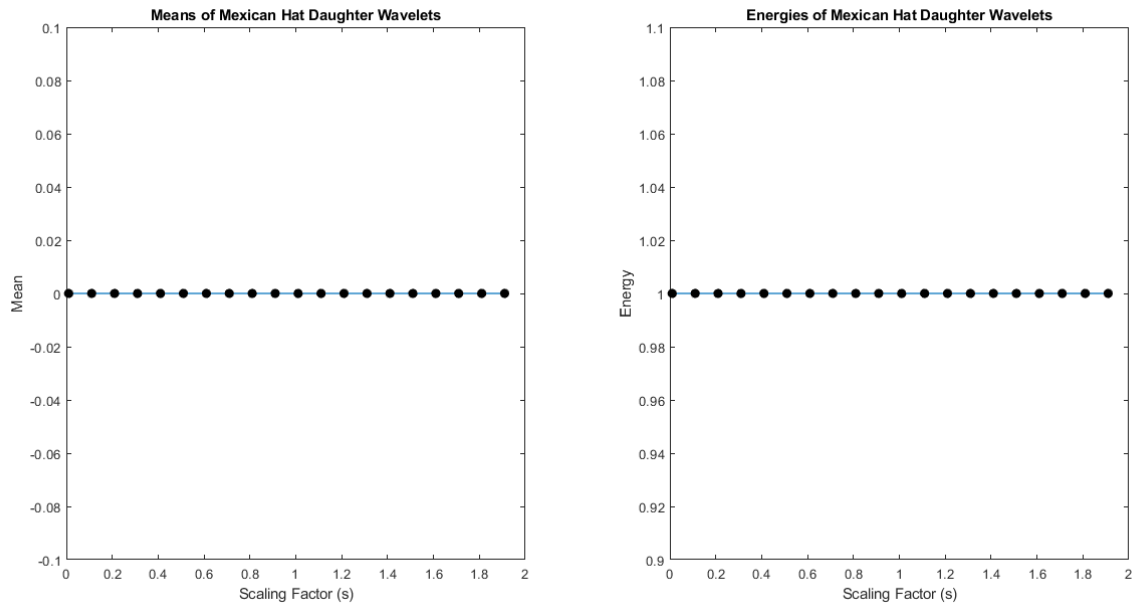


Figure 3: Variation of Means and Energies of Mexican Hat Wavelet Function for Different Scaling Factors

1.2.6 Plotting the Spectra of the Daughter Wavelets

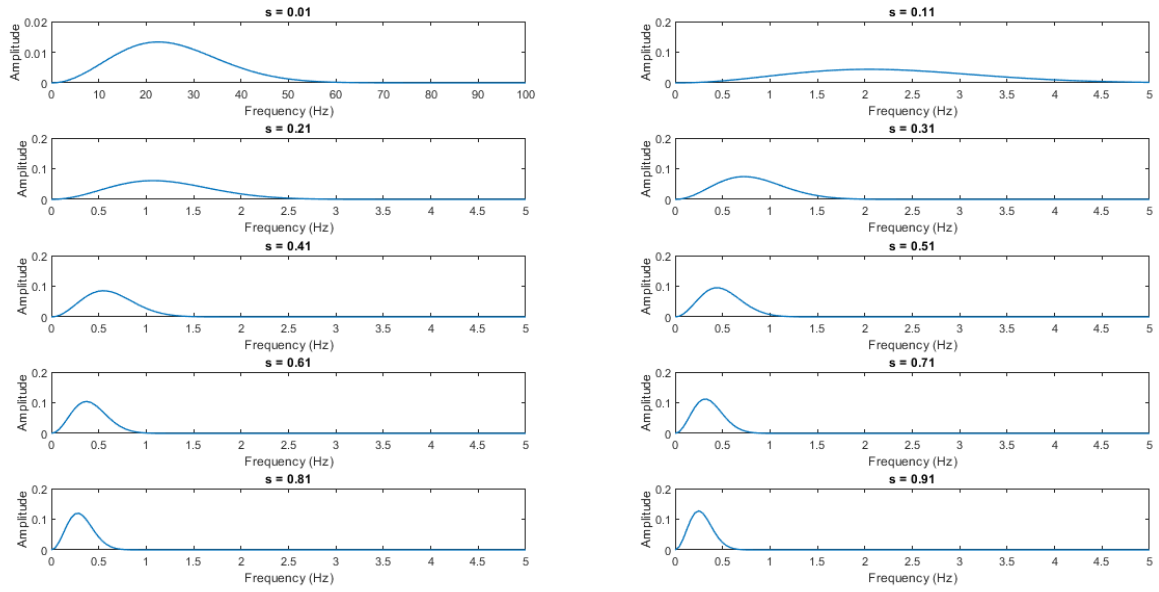


Figure 4: Spectra of the Mexican Hat Daughter Wavelet Function for the first 10 Scaling Factors

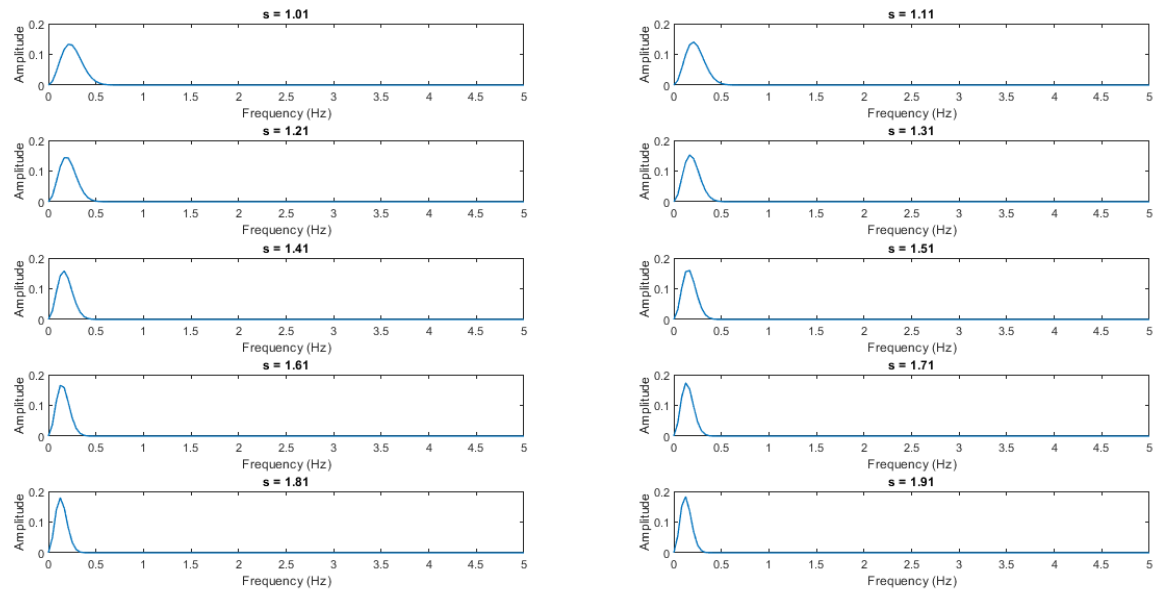


Figure 5: Spectra of the Mexican Hat Daughter Wavelet Function for the last 10 Scaling Factors

As we can see from the above diagrams, the width of the frequency band decreases as we increase the scaling factor. Accordingly, the mean, mode and medians of the frequency band shift to the left as the scaling factor is increased. As all the wavelets have a unity power, this implies that power to the width of the band ratio increases as we increase the scaling factor.

1.3 Continuous Wavelet Decomposition

1.3.1 Creating the Waveform $x[n]$

$$x[n] = \begin{cases} \sin(0.5\pi n) & 1 \leq n < \frac{3N}{2} \\ \sin(1.5\pi n) & \frac{3N}{2} \leq n < 3N \end{cases}$$

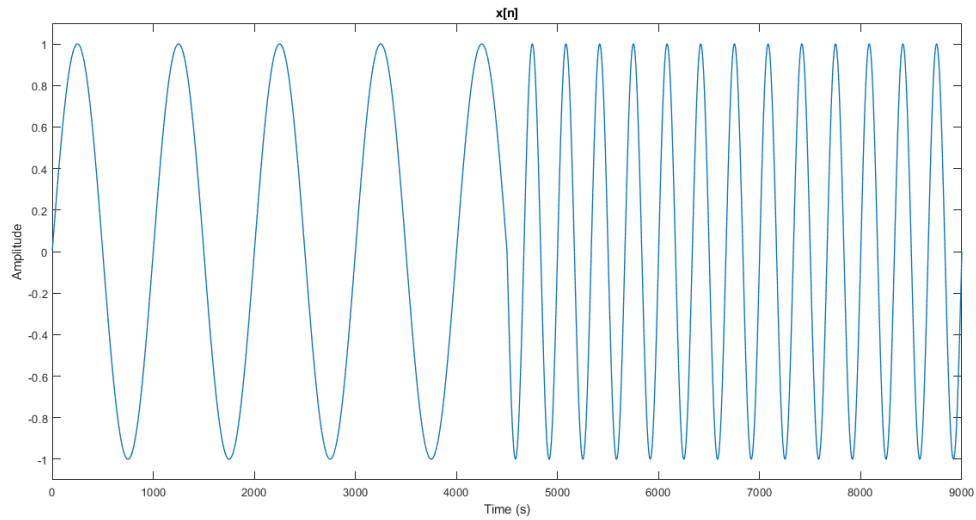


Figure 6: $x[n]$ Signal

1.3.2 Applying the Scaled Mexican Hat Wavelets to $x[n]$

Note: Implemented in the code script: Q1_Assignment3_180497C.m

1.3.3 Visualizing the Spectrogram

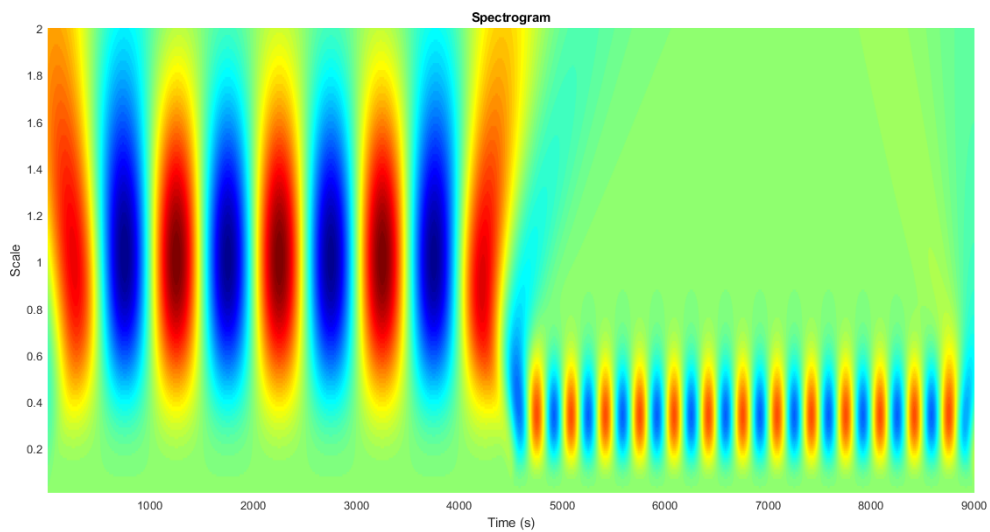


Figure 7: Spectrogram of the $x[n]$ Signal after CWT

1.3.4 Commenting on the Spectrogram

We can observe from the above spectrogram that the higher frequency components are encapsulated by the wavelets with a smaller scaling factor and the lower frequency components are captured by those with a larger scaling factor. This is the expected behaviour because, in part 1.2, we realized that the width of the frequency band of the wavelet decreases when the scaling factor is increased.

Accordingly, when the scaling factor is close to 1, the median frequency is around $0.5\pi \text{ rads}^{-1}$ and it is $1.5\pi \text{ rads}^{-1}$ when the scaling factor is close to 0.4. These are the highlighted regions of the above spectrograms.

2 Discrete Wavelet Transform

2.1 Introduction

In order to overcome the redundant computations involved with CWT, DWT could be used. Let s_0 be the scaling step size and τ_0 be the translation step size. For easier analysis, generally, $s_0 = 2$ and $\tau_0 = 1$. The DWT equation is given below. Note that m and n are multiplier integers.

$$\psi_{m,n}(t) = \frac{1}{\sqrt{s_0^m}} \psi\left(\frac{t - n\tau_0 s_0^m}{s_0^m}\right)$$
$$\psi_{m,n}(t) = \frac{1}{\sqrt{2^m}} \psi\left(\frac{t - 2^m n}{2^m}\right)$$

2.2 Applying DWT with the Wavelet Toolbox in MATLAB

2.2.1 Creating the Waveforms $x_1[n]$ and $x_2[n]$

$$x_1[n] = \begin{cases} 2\sin(20\pi n) + \sin(80\pi n) & 0 \leq n < 512 \\ 0.5\sin(40\pi n) + \sin(60\pi n) & 512 \leq n < 1024 \end{cases}$$

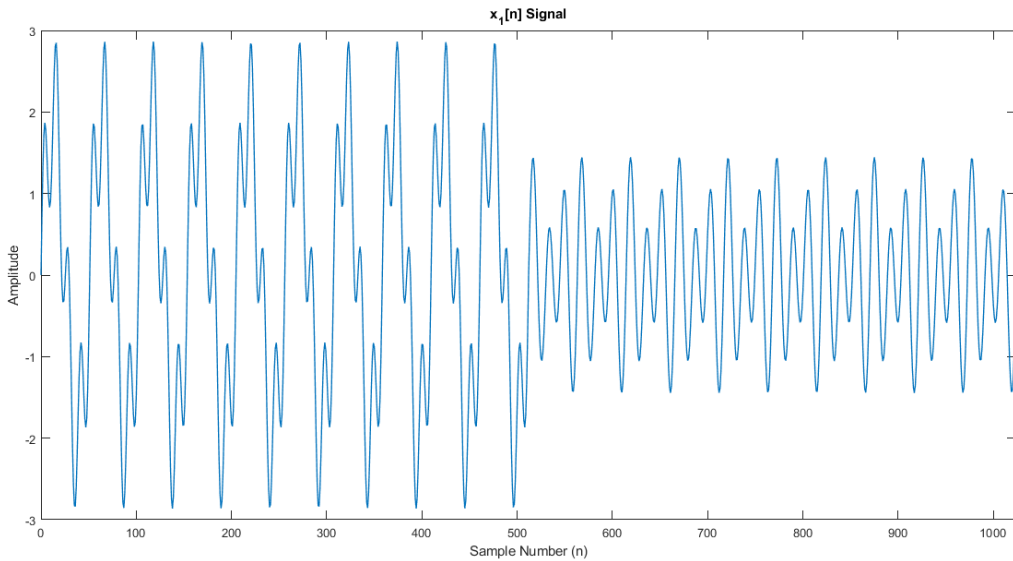


Figure 8: $x_1[n]$ Signal

$$x_2[n] = \begin{cases} 1 & 0 \leq n < 64 \\ 2 & 192 \leq n < 256 \\ -1 & 128 \leq n < 512 \\ 3 & 512 \leq n < 704 \\ 1 & 704 \leq n < 960 \\ 0 & \text{otherwise} \end{cases}$$

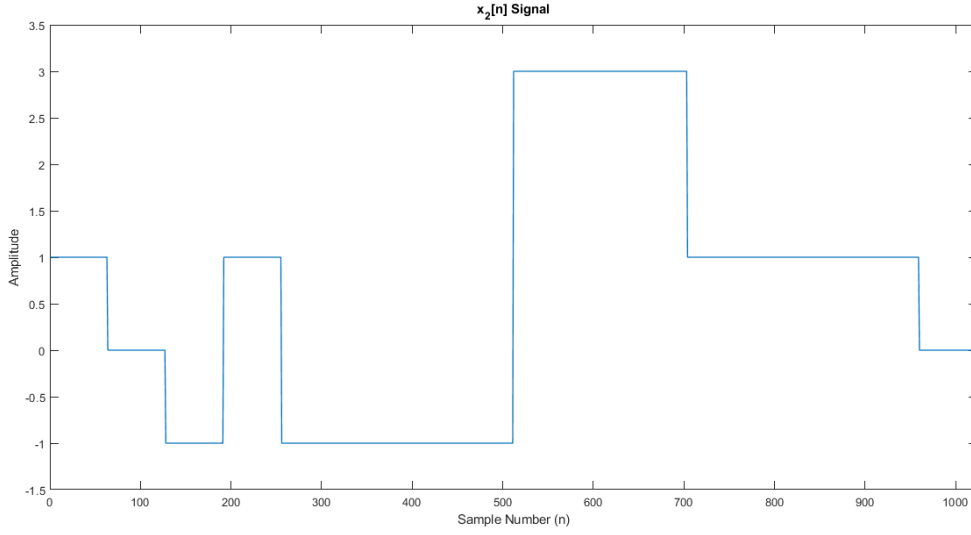


Figure 9: $x_2[n]$ Signal

2.2.1.1 Corrupting $x_1[n]$ and $x_2[n]$ with AWGN

An AWGN of 10dB was added to the $x_1[n]$ and $x_2[n]$ signals and the corrupted noisy signals are called $y_1[n]$ and $y_2[n]$, respectively.

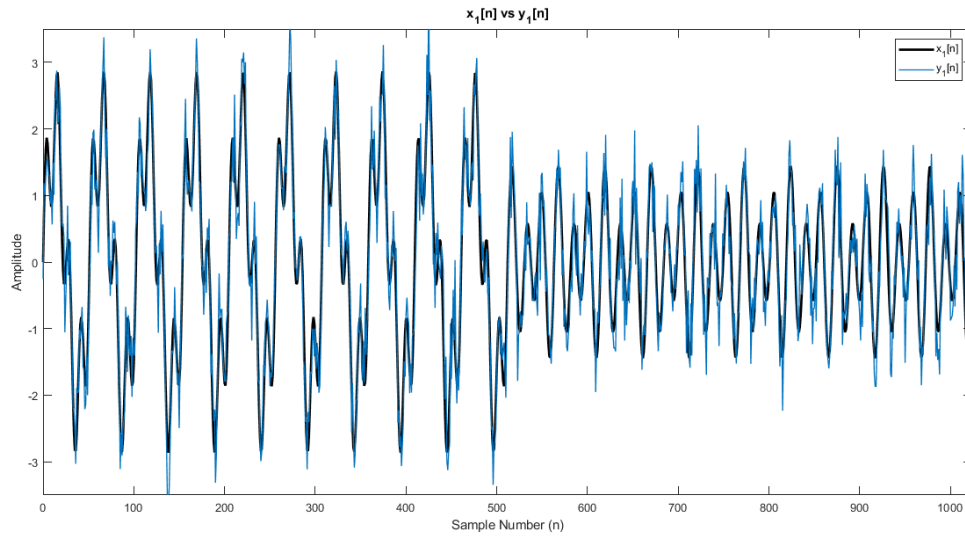


Figure 10: $y_1[n]$ Signal

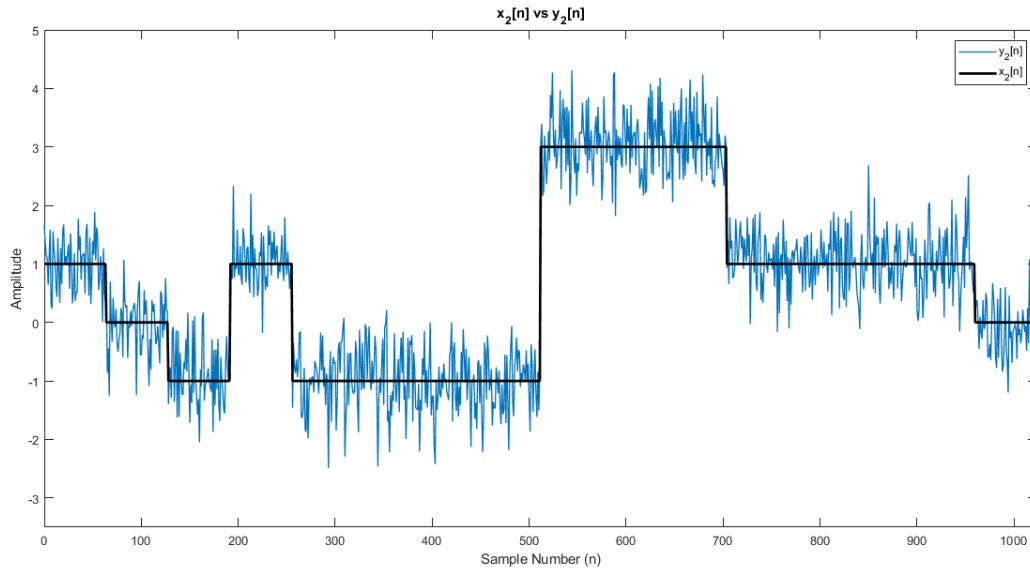


Figure 11: $y_2[n]$ Signal

2.2.2 Observing the Morphology of Haar and Daubechies Tap 9 Wavelets

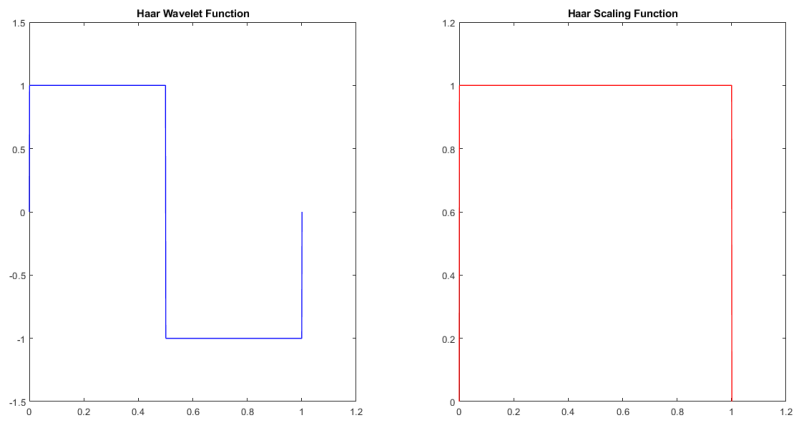


Figure 12: Haar Wavelet Function and Scaling Function (Using wavefun())

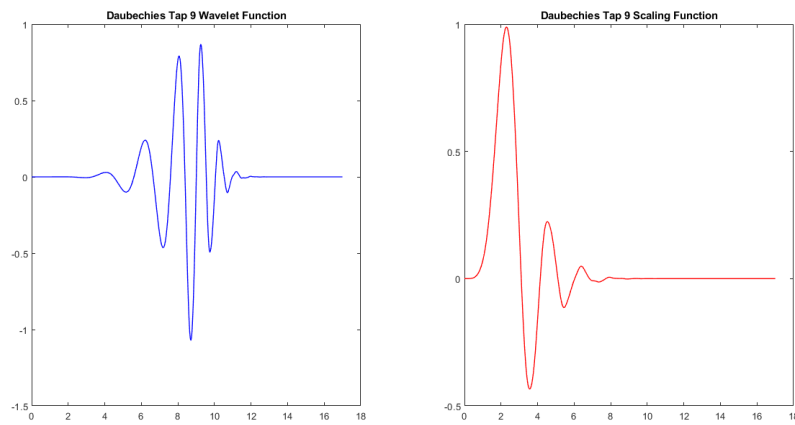


Figure 13: DB-9 Wavelet Function and Scaling Function (Using wavefun())

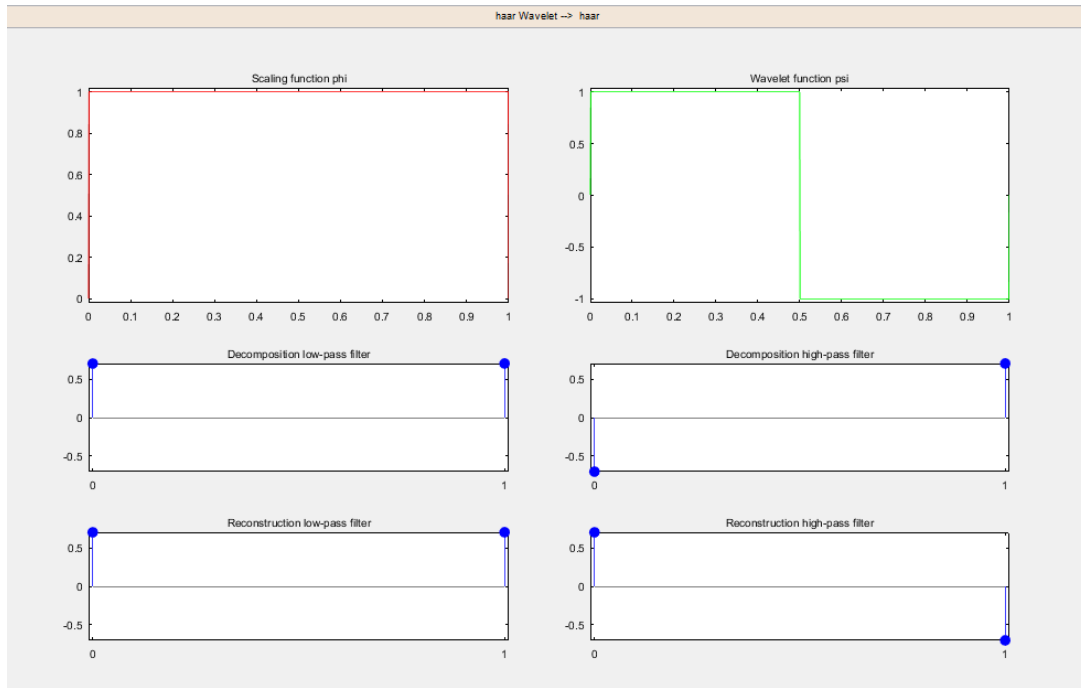


Figure 14: Haar Wavelet Function and Scaling Function (Using waveletAnalyzer GUI)

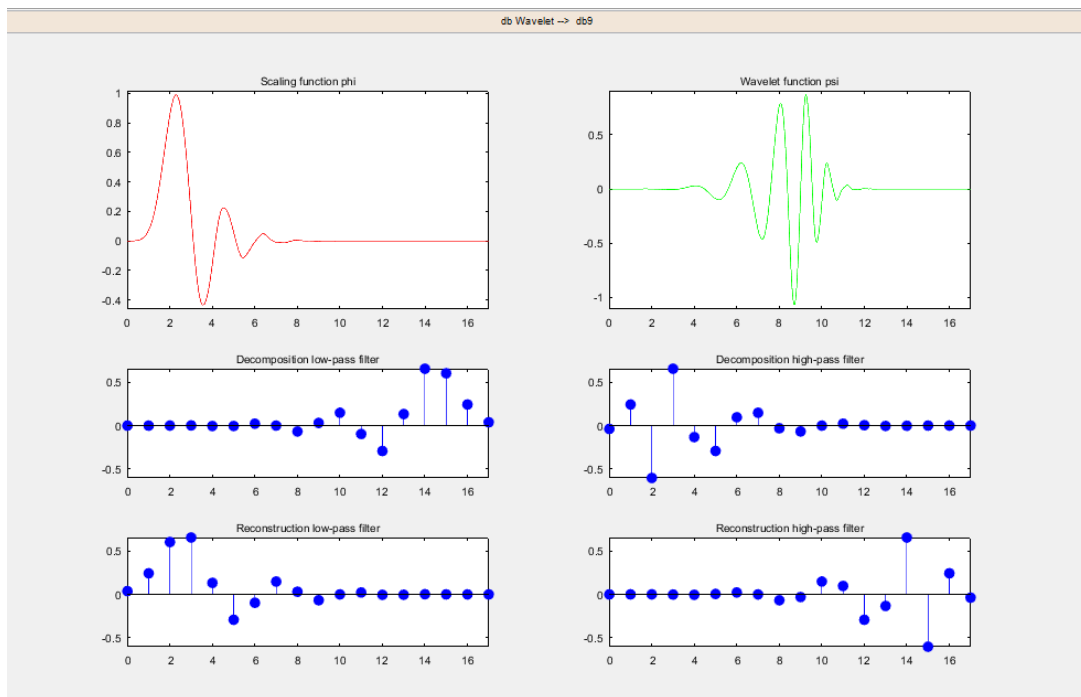


Figure 15: DB-9 Wavelet Function and Scaling Function (Using waveletAnalyzer GUI)

2.2.3 Calculating the 10-level Decomposition of the Signal

2.2.3.1 10-level Decomposition of $y_1[n]$ Signal

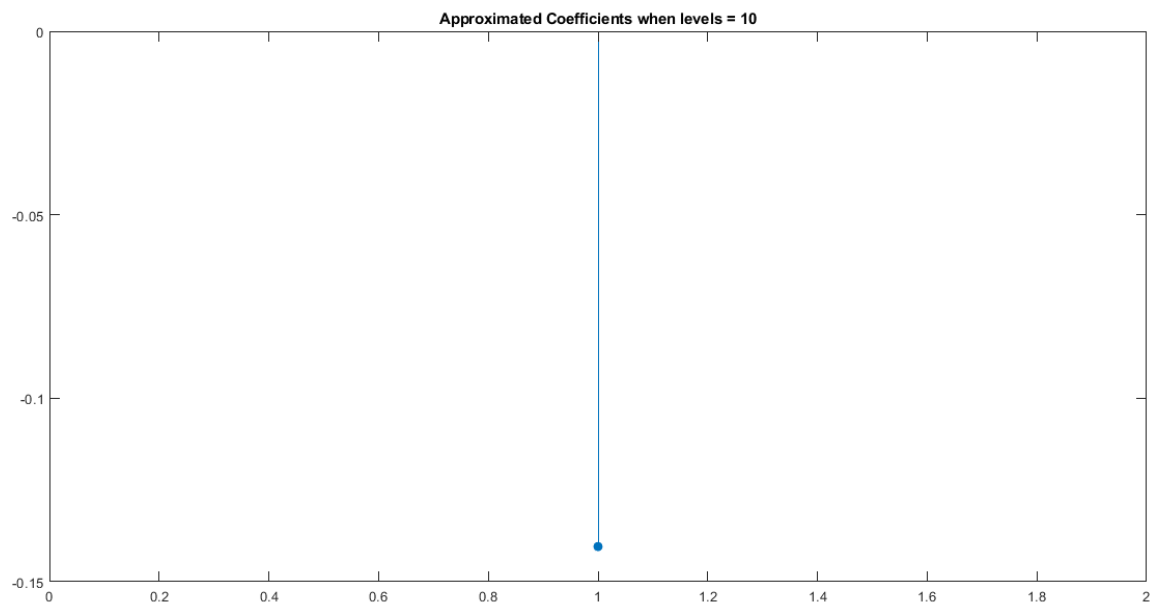


Figure 16: Approximated Coefficients - Haar - 10 Level - $y_1[n]$ Signal

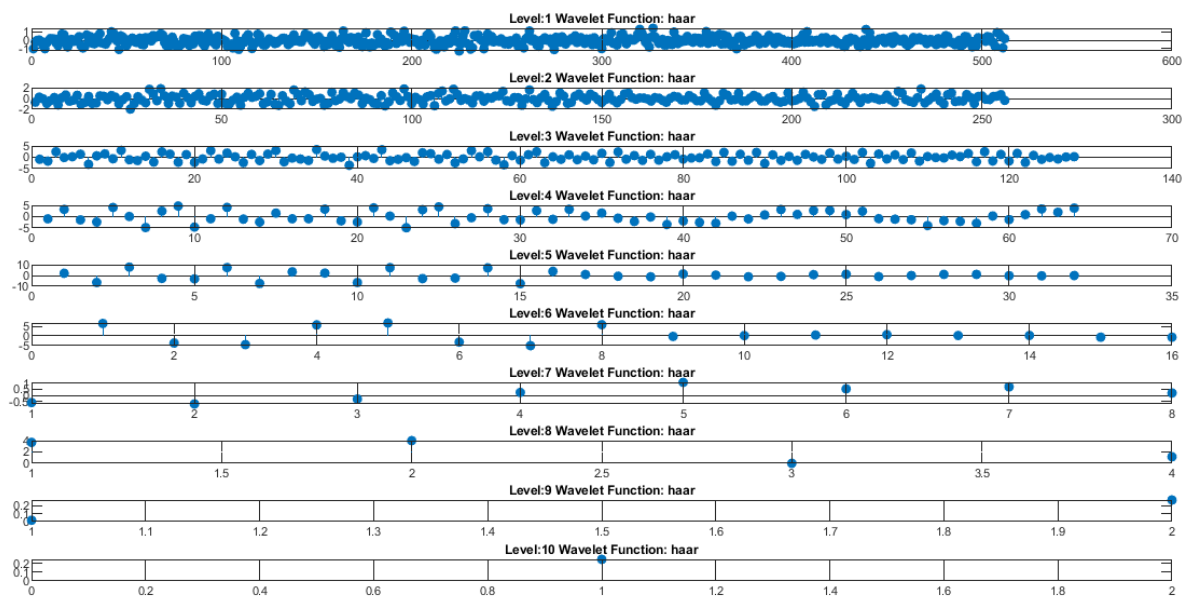


Figure 17: 10-level Decomposition of $y_1[n]$ Signal - Haar Wavelet

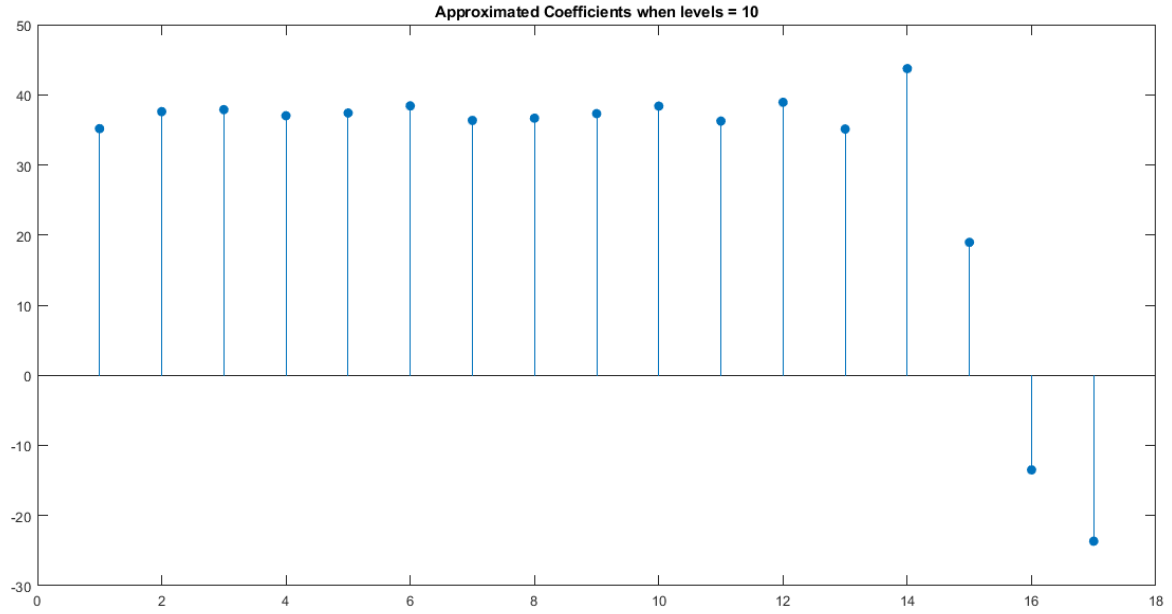


Figure 18: Approximated Coefficients - DB9 - 10 Level - $y_1[n]$ Signal

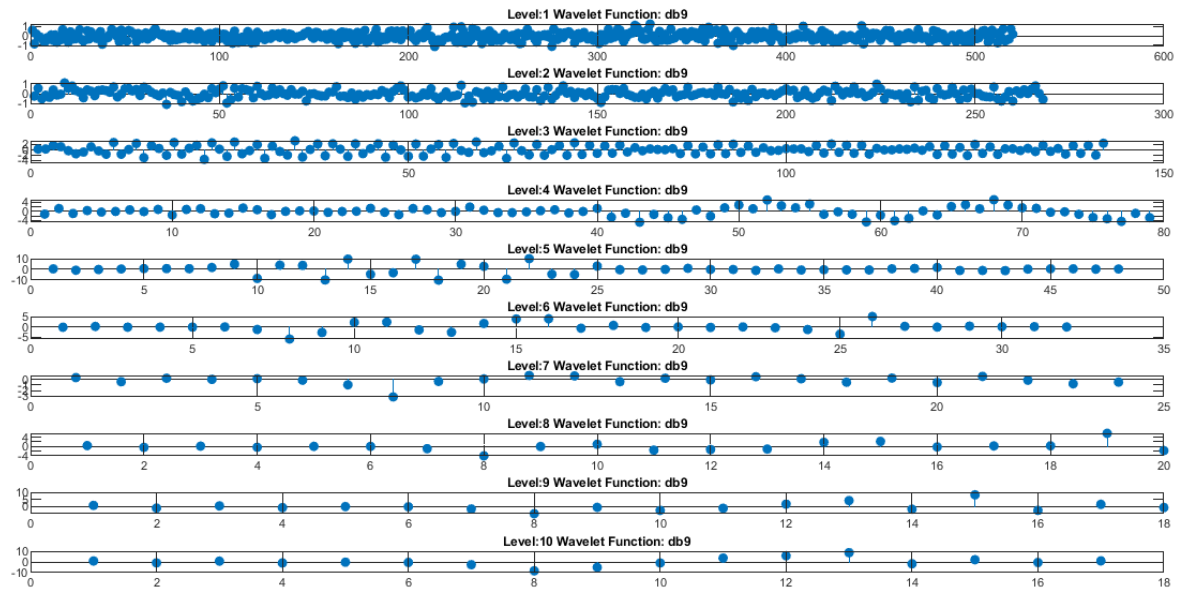


Figure 19: 10-level Decomposition of $y_1[n]$ Signal - DB9 Wavelet

2.2.3.2 10-level Decomposition of $y_2[n]$ Signal

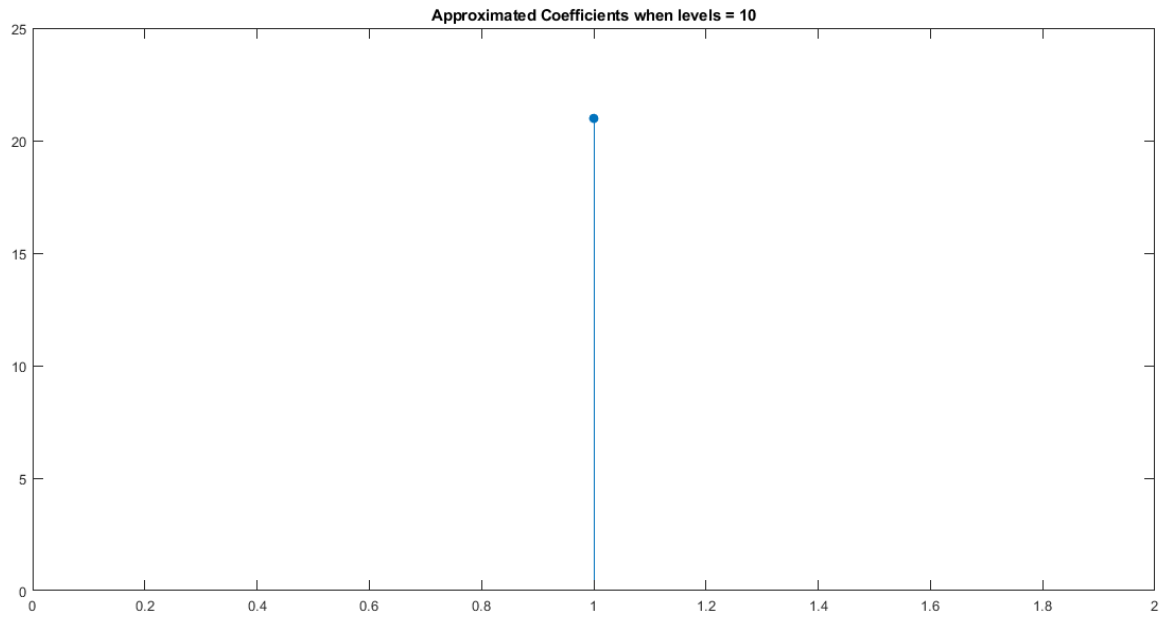


Figure 20: Approximated Coefficients - Haar - 10 Level - $y_2[n]$ Signal

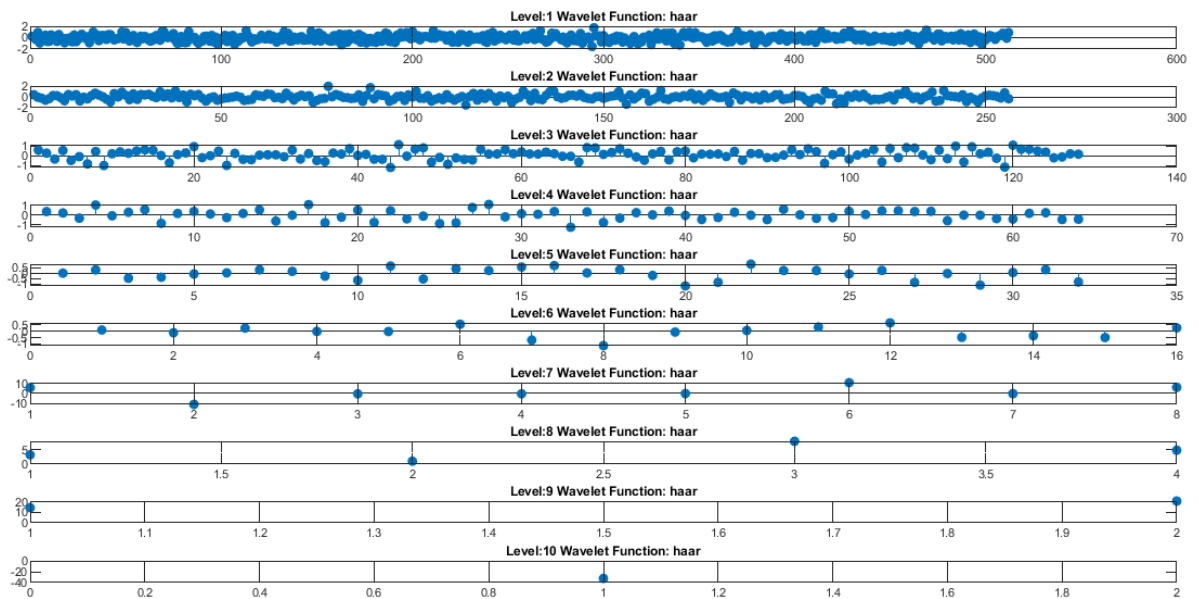


Figure 21: 10-level Decomposition of $y_2[n]$ Signal - Haar Wavelet

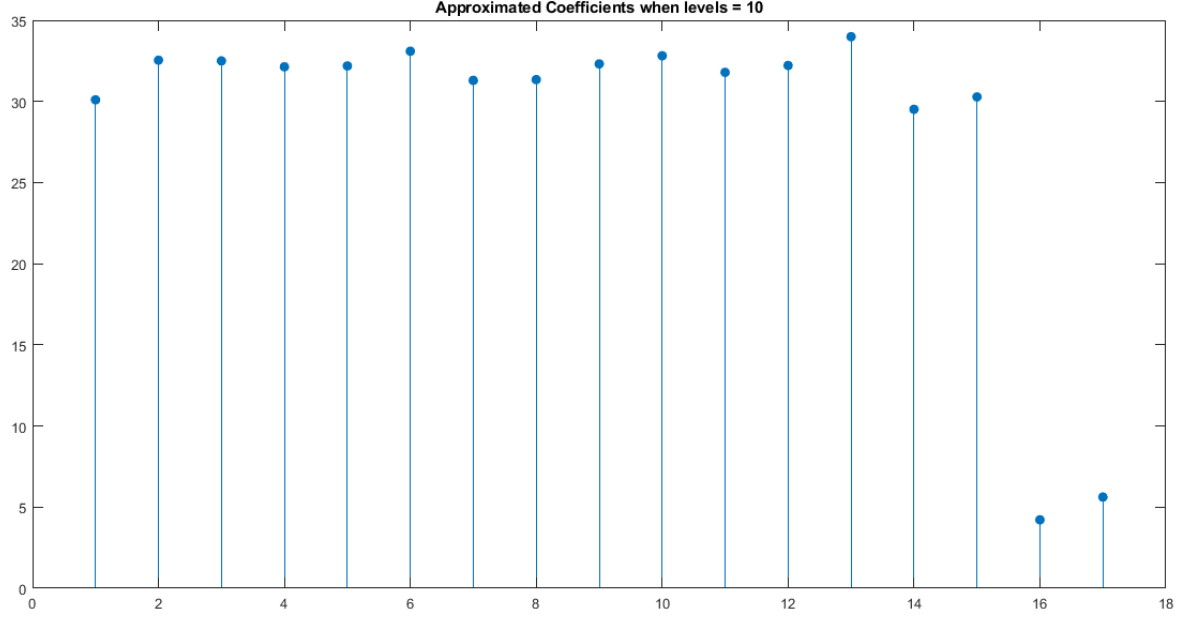


Figure 22: Approximated Coefficients - DB9 - 10 Level - $y_2[n]$ Signal

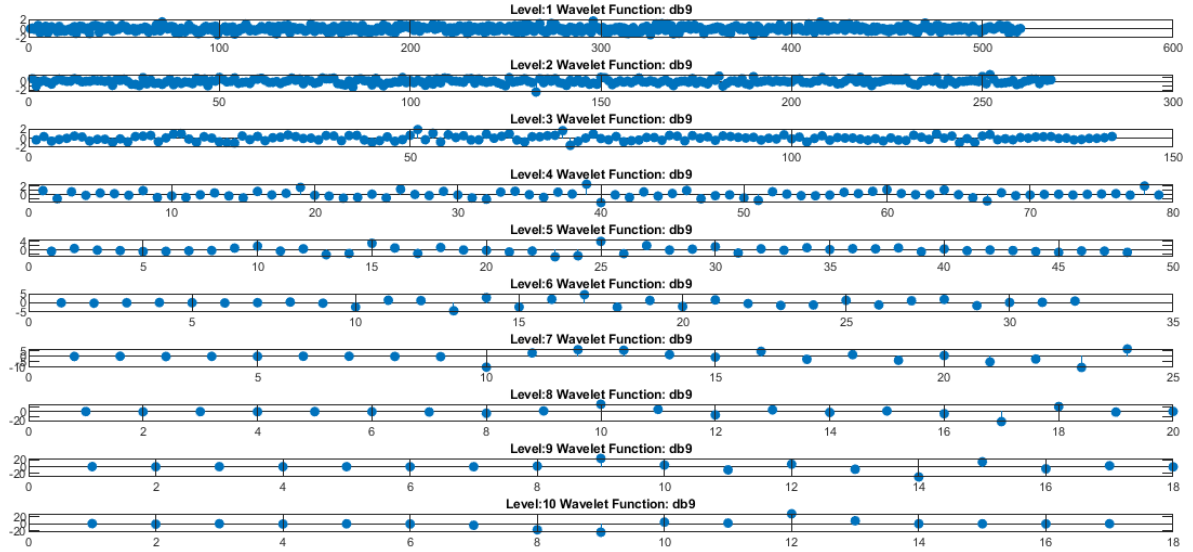


Figure 23: 10-level Decomposition of $y_2[n]$ Signal - DB9 Wavelet

2.2.4 Using Inverse DWT to Reconstruct the Signal

Each detailed function (D) could be used along with the corresponding approximated function (A) to reconstruct the initial noisy signal. Once, the signals are generated, we can compare their energies to verify that $y = \Sigma D^i + A$. The verification is given in the subsequent section.

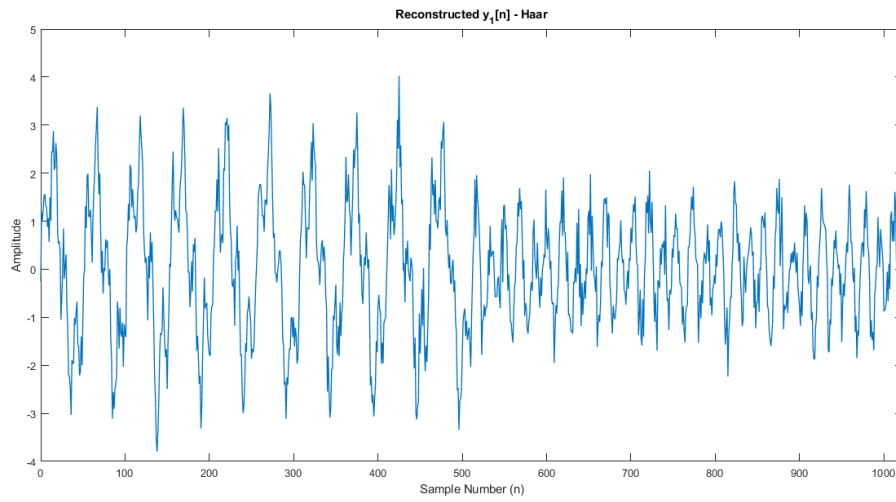


Figure 24: Reconstructed $y_1[n]$ Signal - Haar Wavelet

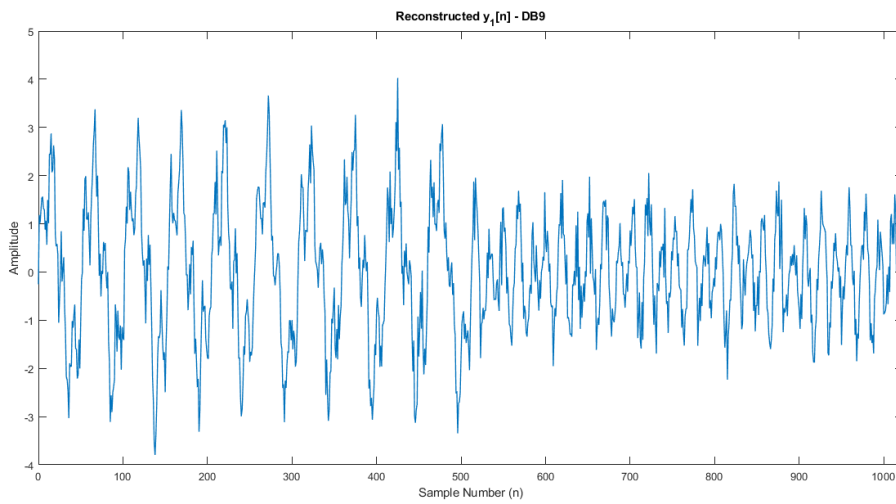


Figure 25: Reconstructed $y_1[n]$ Signal - DB9 Wavelet

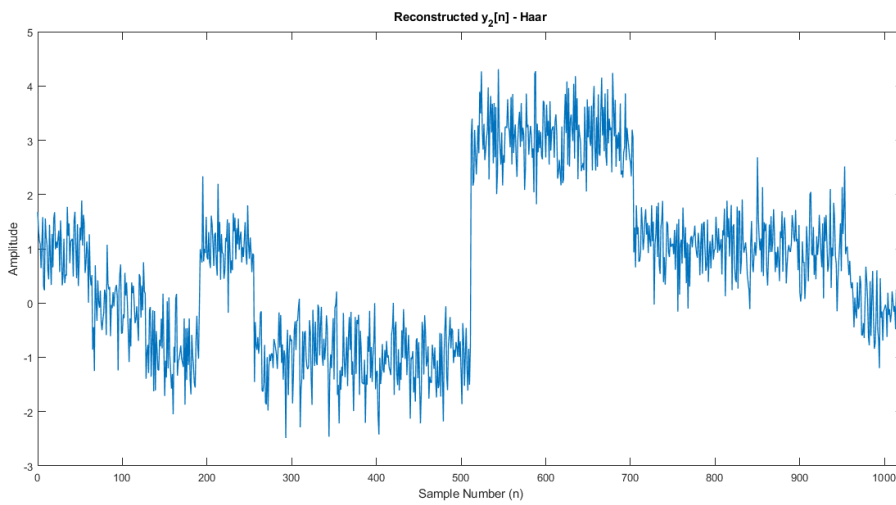


Figure 26: Reconstructed $y_2[n]$ Signal - Haar Wavelet

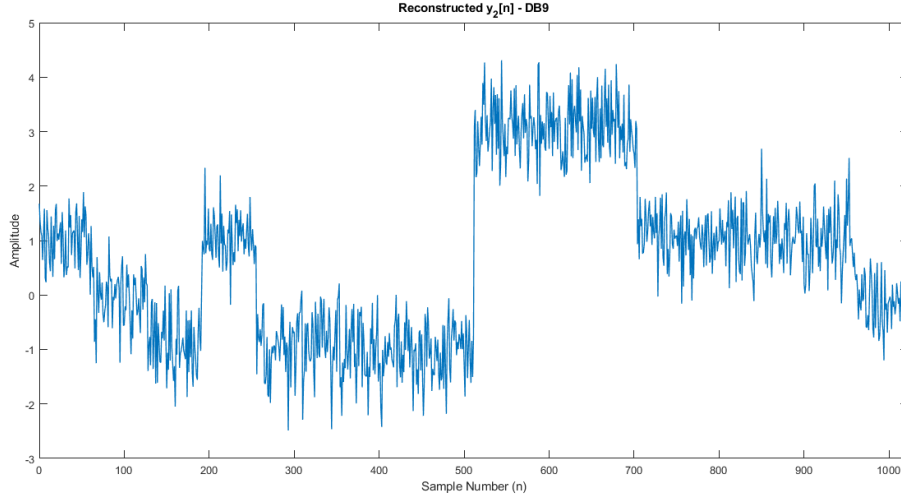


Figure 27: Reconstructed $y_2[n]$ Signal - DB9 Wavelet

2.2.4.1 Comparing the Energies the Original and Reconstructed Noisy Signals

The following tables summarize the energies of the initial noisy signals and the reconstructed signals.

Signal	Energy
Original $y_1[n]$ Signal	1722.4
Reconstructed $y_1[n]$ Signal (Haar)	1722.4
Reconstructed $y_1[n]$ Signal (DB9)	1722.4

Table 1: Energy Comparison between Original and Reconstructed $y_1[n]$ Signals

Signal	Energy
Original $y_2[n]$ Signal	2800.5
Reconstructed $y_2[n]$ Signal (Haar)	2800.5
Reconstructed $y_2[n]$ Signal (DB9)	2800.5

Table 2: Energy Comparison between Original and Reconstructed $y_2[n]$ Signals

Energy calculations are provided in the MATLAB script Q2_Assignment3_180497C.m

2.3 Signal Denoising with DWT

Note that the solutions for question 2.3.4 (repeating for Haar Wavelet) are also combined with the solutions of questions 2.3.1, 2.3.2, and 2.3.3, for better comparison.

2.3.1 Plotting the Magnitudes of the Wavelet Coefficients

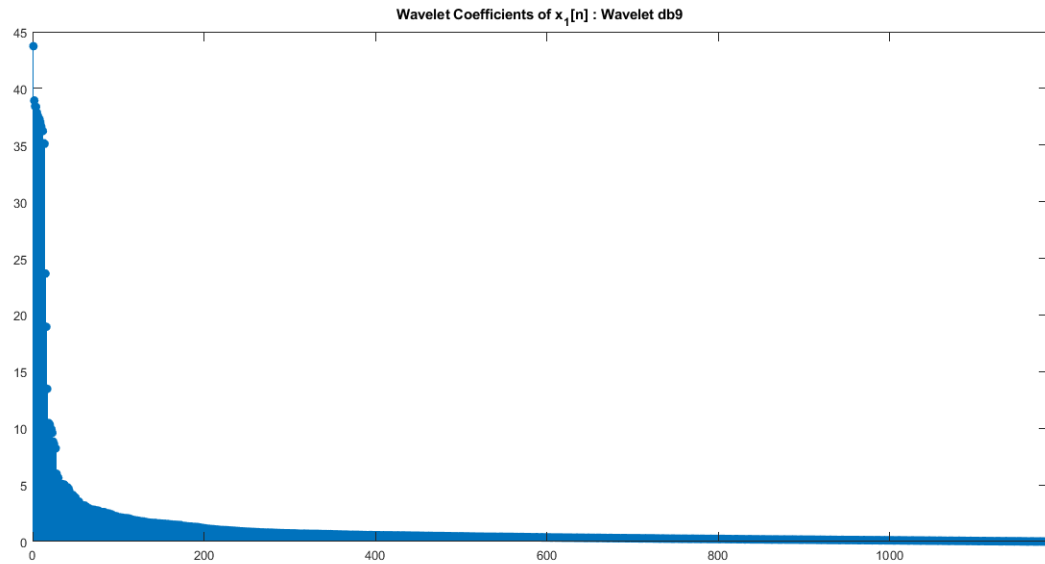


Figure 28: Wavelet Coefficients for the First Wave Pair - DB9 Wavelet

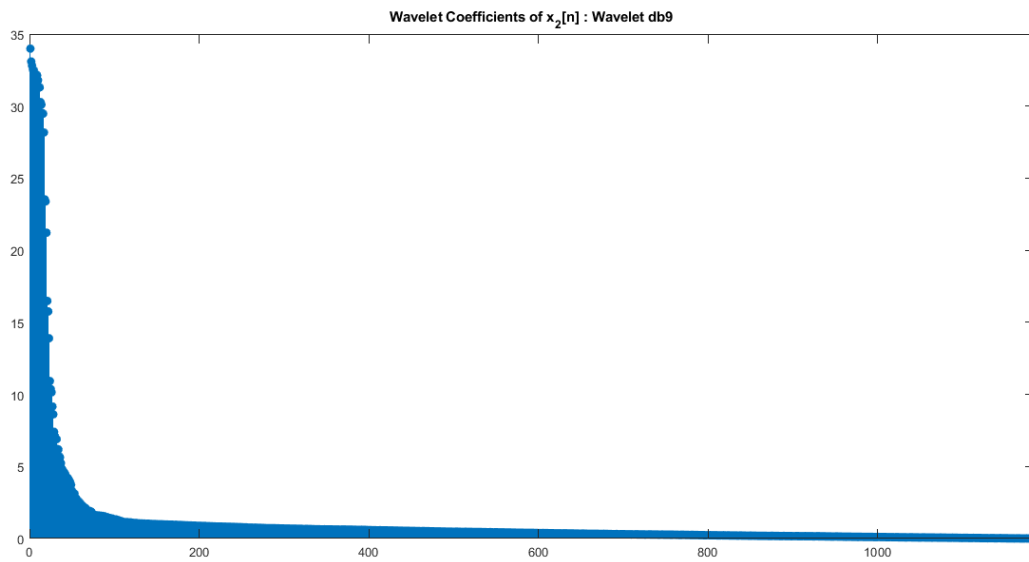


Figure 29: Wavelet Coefficients for the Second Wave Pair - DB9 Wavelet

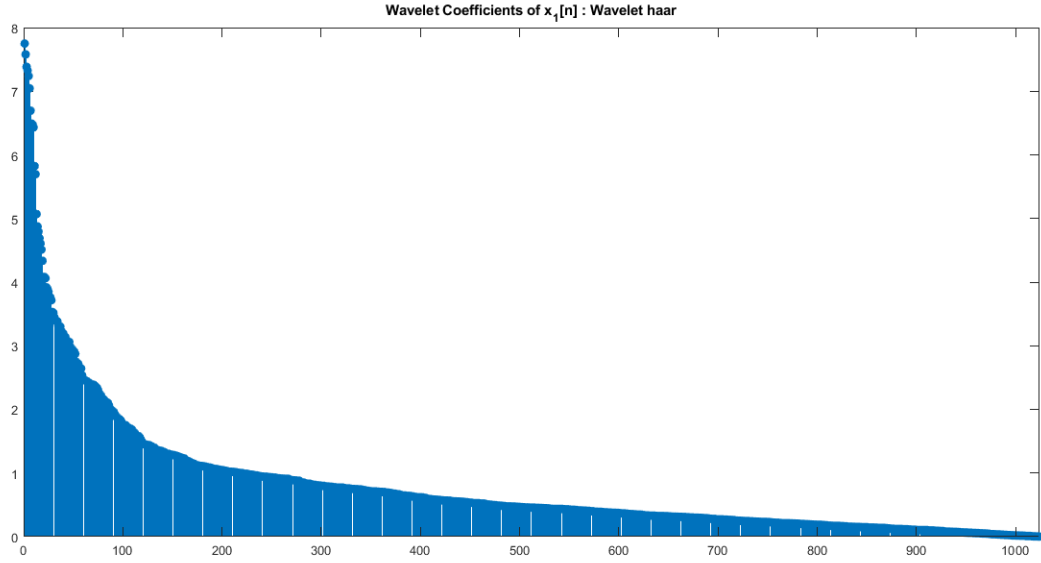


Figure 30: Wavelet Coefficients for the First Wave Pair - Haar Wavelet

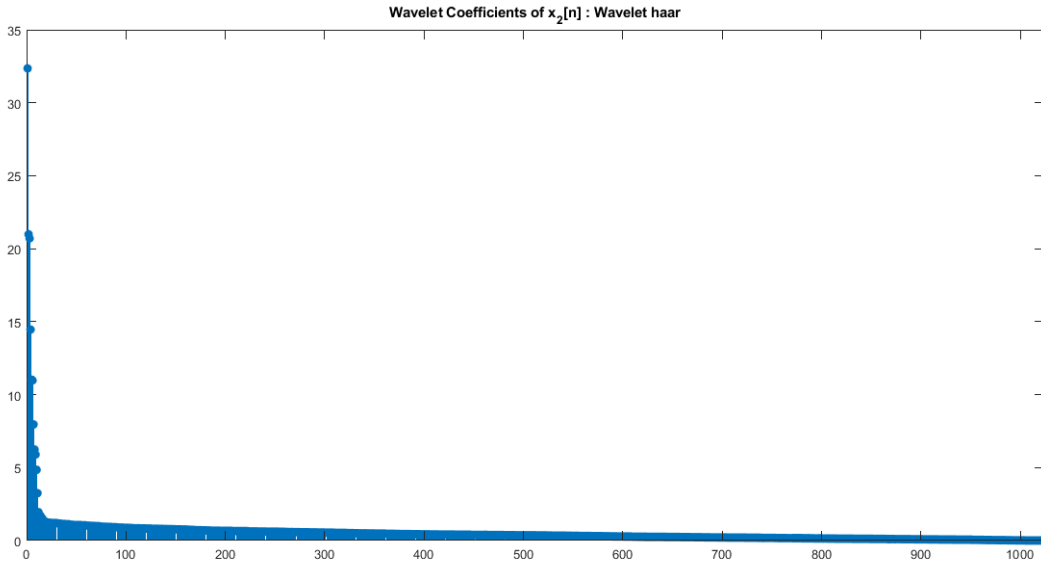


Figure 31: Wavelet Coefficients for the Second Wave Pair - Haar Wavelet

2.3.2 Selecting Thresholds and Reconstructing the Signals

After observing the two pairs of signals; $\{x_1[n], y_1[n]\}$ and $\{x_2[n], y_2[n]\}$, following thresholds were selected to yield a smaller RMSE. The values were handpicked after trying out some threshold values, manually.

- Threshold for the first pair of waves $\{x_1[n], y_1[n]\}$: 0.85
- Threshold for the second pair of waves $\{x_2[n], y_2[n]\}$: 1.95

After using the above thresholds, we can obtain the following denoised signals.

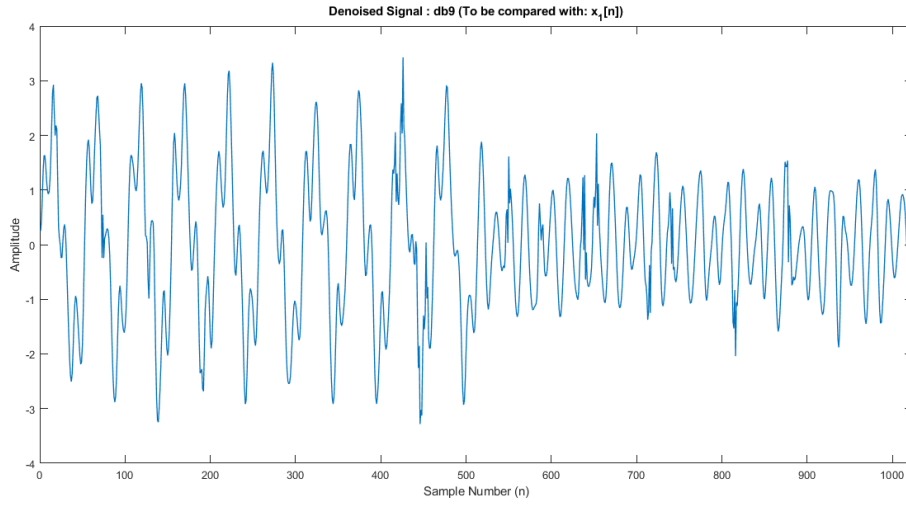


Figure 32: Denoised $y_1[n]$ Signal - DB9 Wavelet

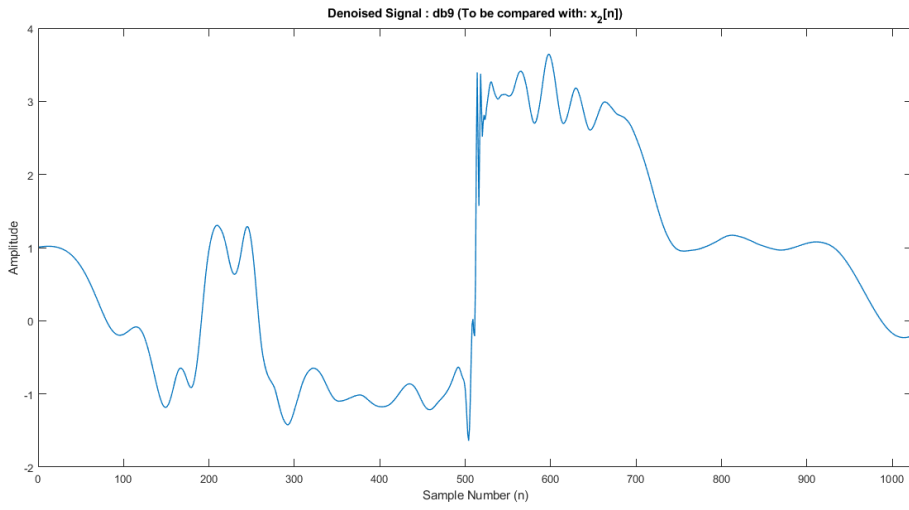


Figure 33: Denoised $y_2[n]$ Signal - DB9 Wavelet

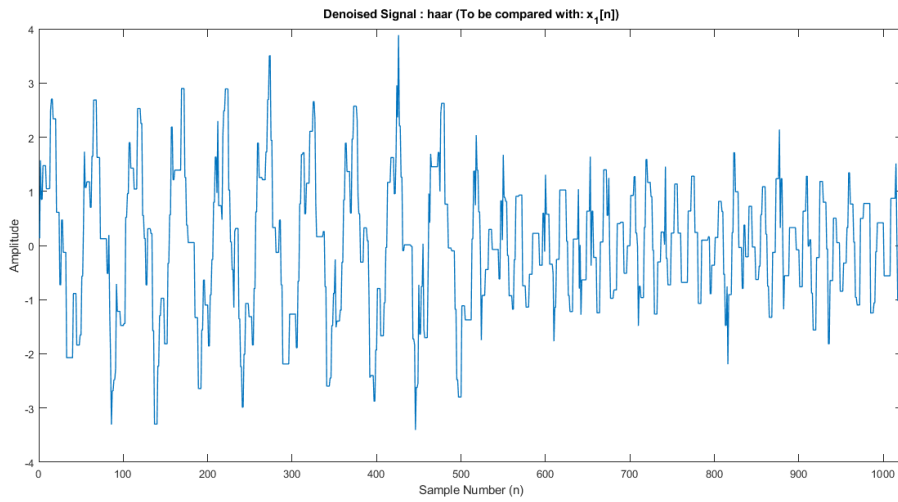


Figure 34: Denoised $y_1[n]$ Signal - Haar Wavelet

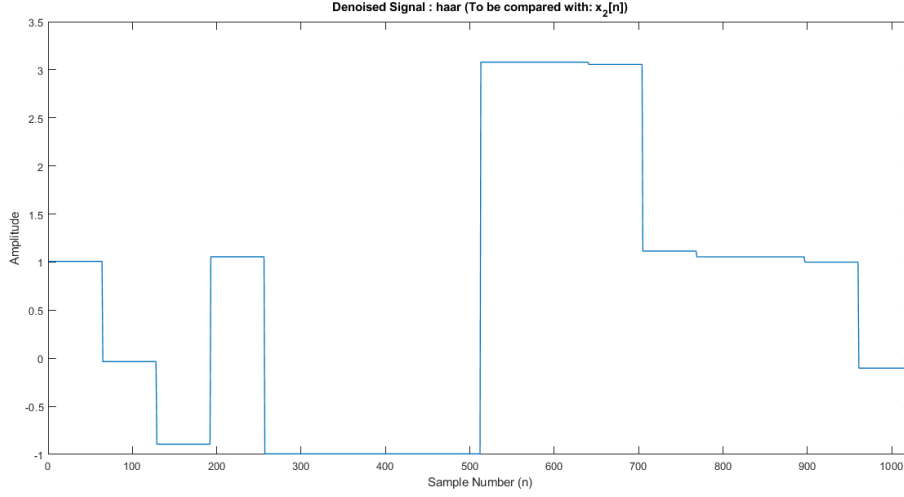


Figure 35: Denoised $y_2[n]$ Signal - Haar Wavelet

2.3.3 Calculating the RMSE between the Original Signal and Denoised Signal

The following table summarizes the RMSE values obtained for the two pairs of waves under the DB9 and Haar Wavelets.

Wave Pair	Wavelet	RMSE
$x_1[n]$ and Denoised $y_1[n]$	DB9	0.2593
$x_1[n]$ and Denoised $y_1[n]$	Haar	0.4134
$x_2[n]$ and Denoised $y_2[n]$	DB9	0.2871
$x_1[n]$ and Denoised $y_1[n]$	Haar	0.0618

Table 3: Comparson between the RMSEs under Haar and DB9 Wavelets

From the above table, we can see that the DB9 wavelet provides better results when the original signal is periodic whereas the Haar wavelet has performed better under a piecewise continuous signal with sudden transitions.

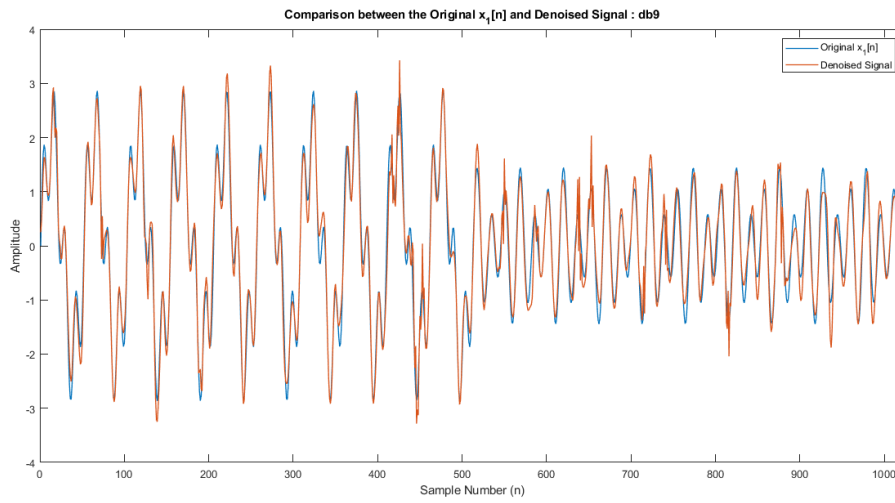


Figure 36: $x_1[n]$ Signal and Denoised $y_1[n]$ Signal - DB9 Wavelet

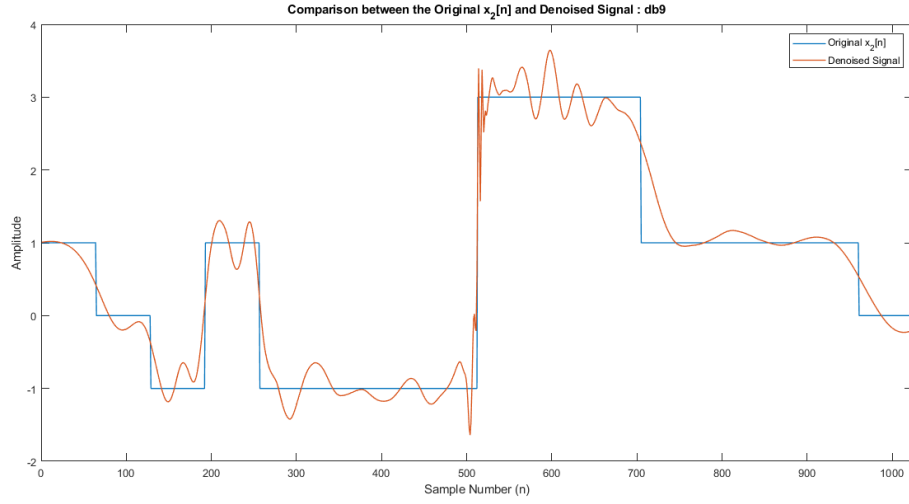


Figure 37: $x_2[n]$ Signal and Denoised $y_2[n]$ Signal - DB9 Wavelet

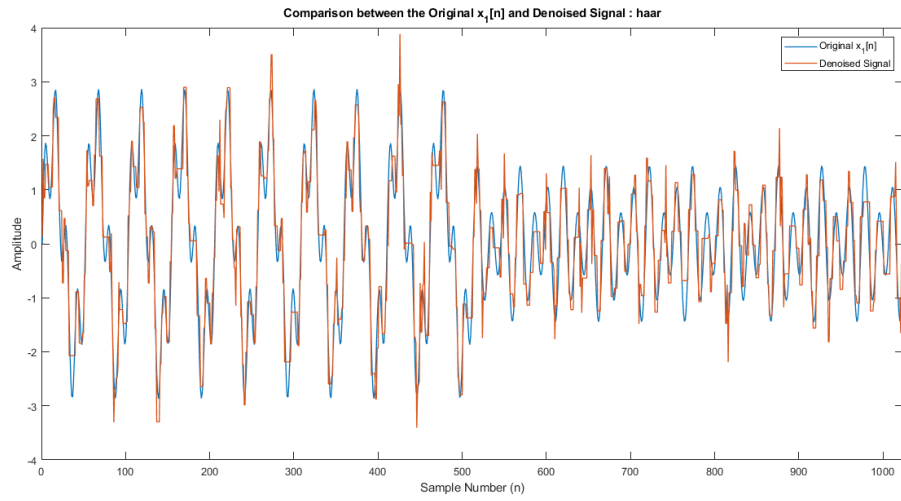


Figure 38: $x_1[n]$ Signal and Denoised $y_1[n]$ Signal - Haar Wavelet

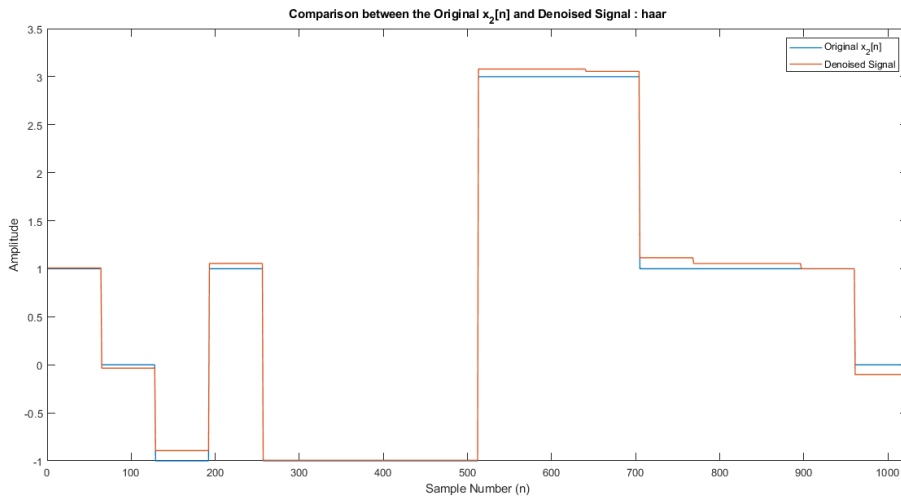


Figure 39: $x_2[n]$ Signal and Denoised $y_2[n]$ Signal - Haar Wavelet

2.3.4 Repeating the Procedure with Haar Wavelets

All the results and explanations for this section are provided under the previous three sections for a better comparison.

2.3.5 Commenting on the Suitability of the Wavelets used

From Table 3, we observed that the Haar wavelet is more suitable when the original signal corresponding to the noisy signal is a piecewise continuous signal with sudden transitions at certain time steps. On the other hand, it was evident that the Daubechies tap 9 wavelet is suitable when the signal corresponding to the noisy signal is a periodic signal, preferably a sinusoid or a combination of sinusoidal signals.

2.4 Signal Compression with DWT

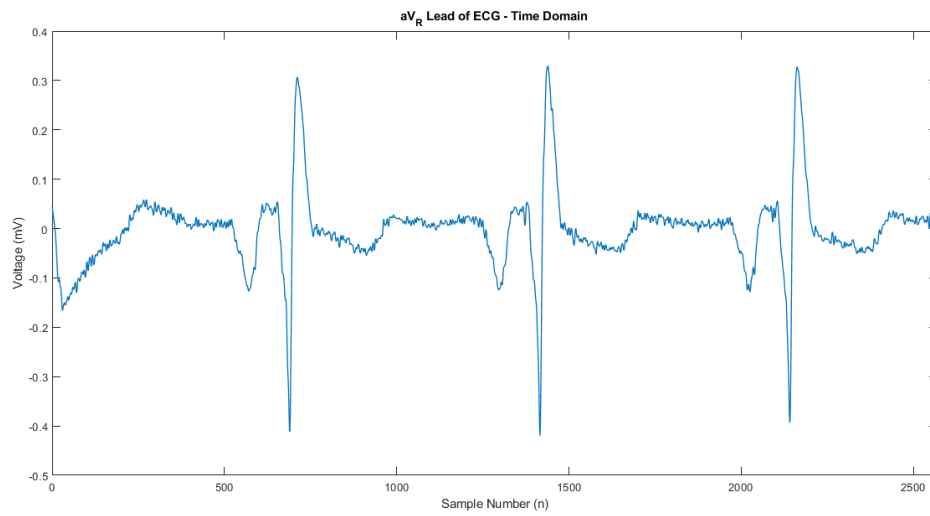


Figure 40: aV_R Lead of ECG

2.4.1 Obtaining the Discrete Wavelet Coefficients of the ECG Signal

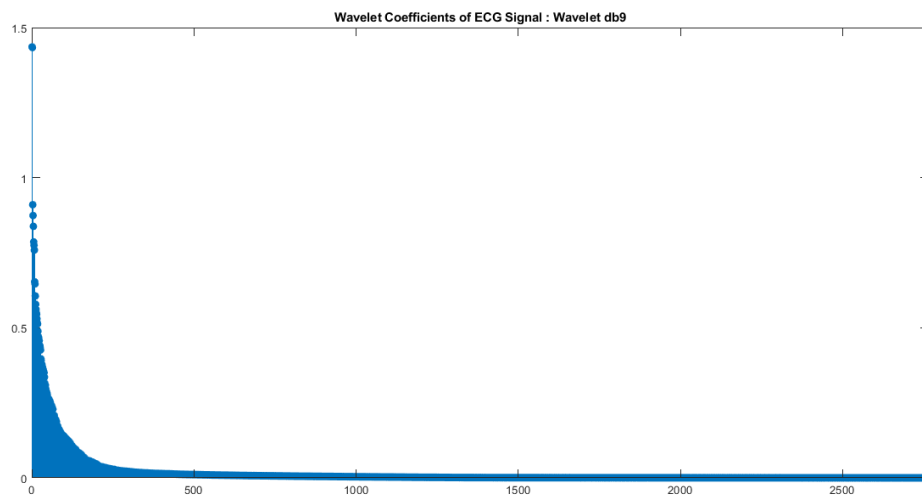


Figure 41: Wavelet Coefficients of the ECG Signal: DB9 Wavelet

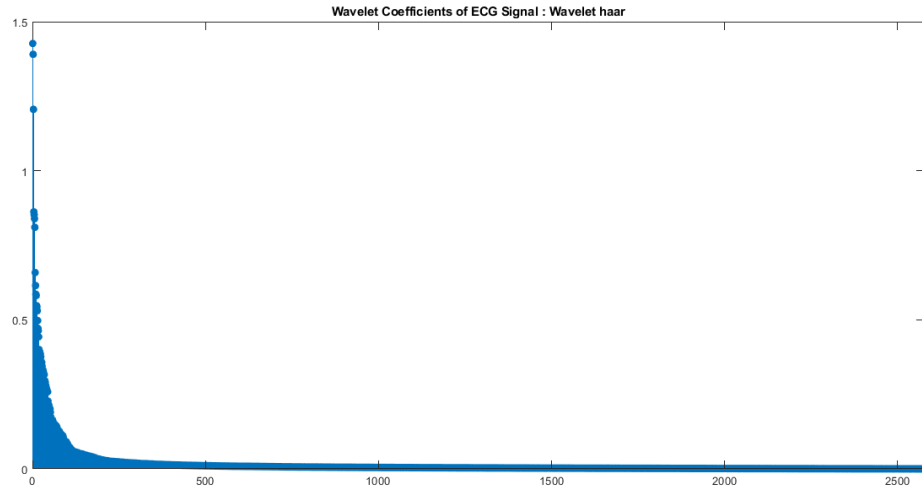


Figure 42: Wavelet Coefficients of the ECG Signal: Haar Wavelet

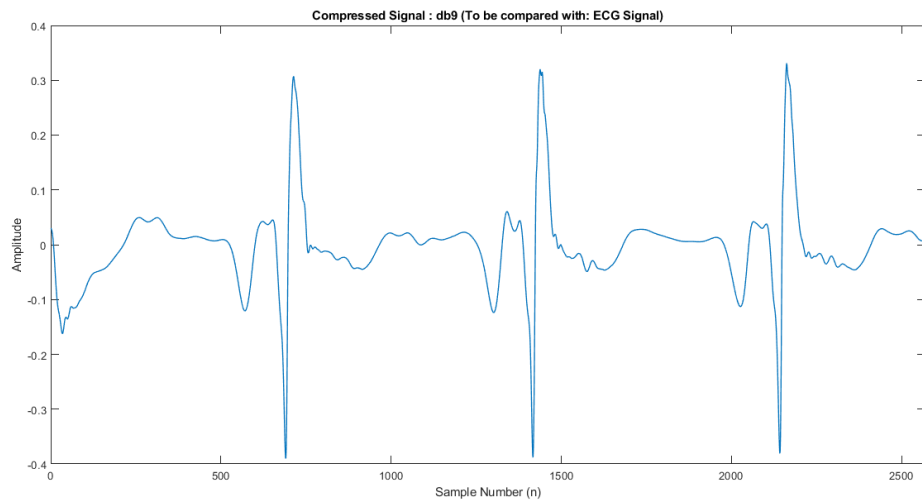


Figure 43: Compressed ECG Signal: DB9 Wavelet

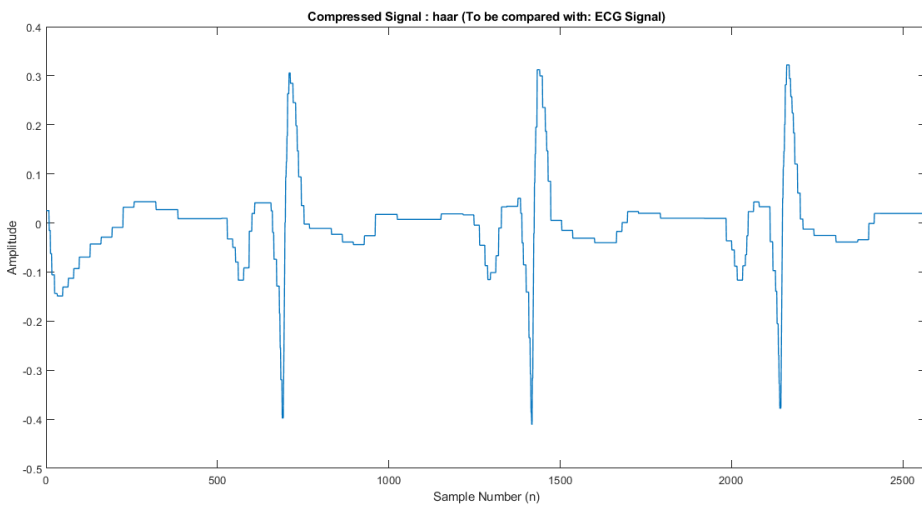


Figure 44: Compressed ECG Signal: Haar Wavelet

2.4.2 Finding the no. of Coefficients which Represent 99% of the Energy

The following table summarizes the results from the analysis that was performed to determine the no. of coefficients that captures 99% of the energy.

Wavelet Function	No. of Coefficients
Daubechies Tap 9	161
Haar	138

Table 4: No. of Coefficients which Represent 99% of the Energy

2.4.3 Compressing the ECG Signal and Finding the Compression Ratio

2.4.3.1 Using the DB9 Wavelet

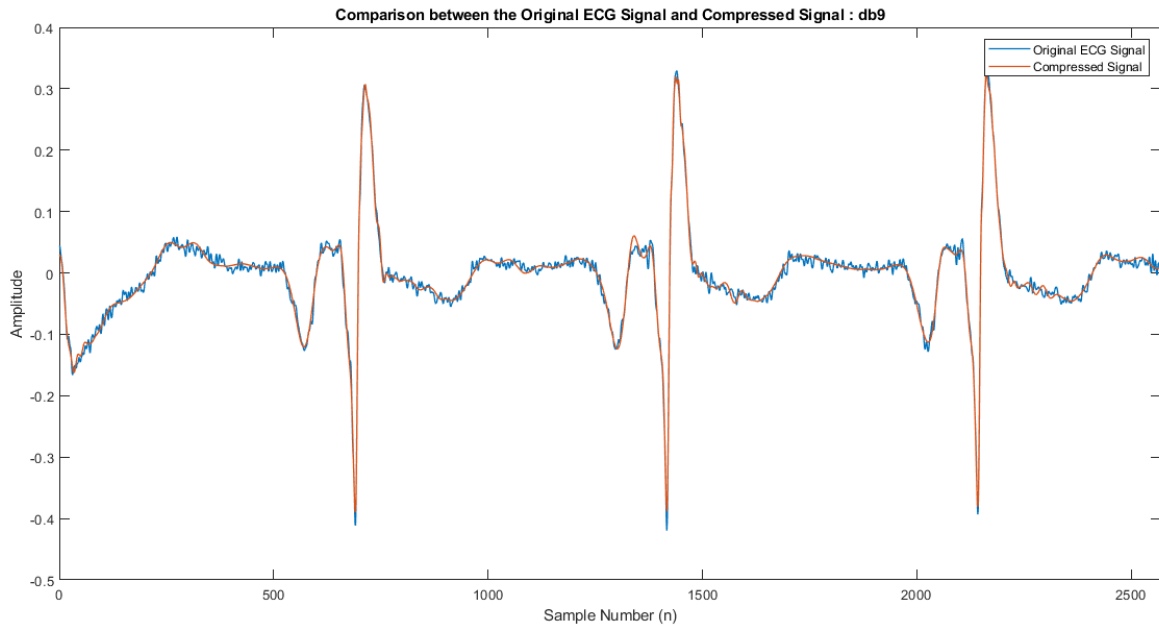


Figure 45: Original and Compressed ECG Signal: DB9 Wavelet

Uncompressed Data Size	2570
No. of Levels Used	$\lceil \log_2(2570) \rceil = 12$
No. of Significant Coefficients	161
Compressed Data Size	173
Compression Ratio	$\frac{2570}{173} = 14.86$
RMSE	0.0081

Table 5: Summary of Compression Results: DB9 Wavelet

The usage of the DB9 wavelet has resulted in a reasonable compression ratio of 14.86 with a satisfactory RMSE of 0.0081. Owing to the smaller RMSE, we could observe that the compressed signal resembles the original ECG signal to a greater extent.

2.4.3.2 Using the Haar Wavelet

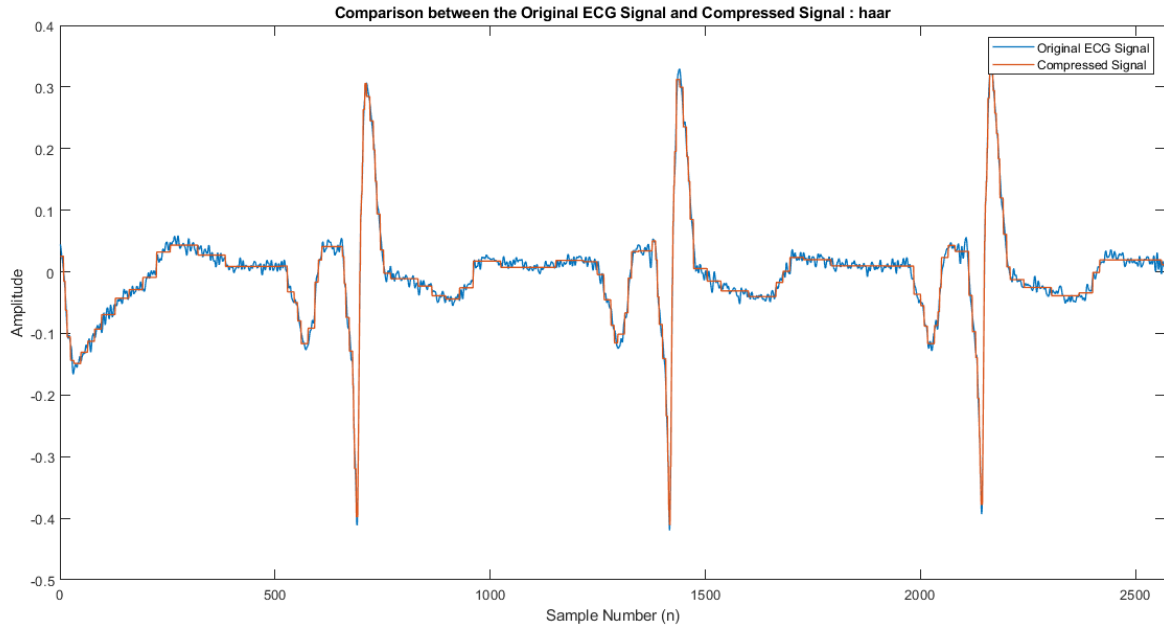


Figure 46: Original and Compressed ECG Signal: Haar Wavelet

Uncompressed Data Size	2570
No. of Levels Used	$\lceil \log_2(2570) \rceil = 12$
No. of Significant Coefficients	138
Compressed Data Size	150
Compression Ratio	$\frac{2570}{150} = 17.13$
RMSE	0.0096

Table 6: Summary of Compression Results: Haar Wavelet

The usage of the Haar wavelet has resulted in a better compression ratio of 17.13 with a relatively higher RMSE of 0.0096 (compared to DB9 wavelet case). Accordingly, the Haar wavelet has managed to compress the ECG signal more than the DB9 wavelet and as expected RMSE from the Haar wavelet is slightly greater than that from the DB9 wavelet.